Hot-Electron Temperature and Laser-Light Absorption in Fast Ignition

M. G. Haines,[1,2] M. S. Wei,[2] F. N. Beg,[2,*] and R. B. Stephens[3]
[1]Physics Department, Imperial College, London, SW7 2AZ, United Kingdom
[2]University of California, San Diego, 9500 Gilman Drive, La Jolla, California 92093-0411, USA
[3]General Atomics, P.O. Box 85608, San Diego, California 92186-5608, USA
(Received 16 May 2008; published 30 January 2009)

Experimental data [F. N. Beg *et al.*, Phys. Plasmas **4**, 447 (1997)] indicate that for intense short-pulse laser-solid interactions at intensities up to $5 \times 10^{18}\ \mathrm{W\,cm^{-2}}$ the hot-electron temperature $\propto (I\lambda^2)^{1/3}$. A fully relativistic analytic model based on energy and momentum conservation laws for the laser interaction with an overdense plasma is presented here. A general formula for the hot-electron temperature is found that closely agrees with the experimental scaling over the relevant intensity range. This scaling is much lower than ponderomotive scaling. Examination of the electron forward displacement compared to the collisionless skin depth shows that electrons experience only a fraction of a laser-light period before being accelerated forward beyond the laser light's penetration region. Inclusion of backscattered light in a modified model indicates that light absorption approaches 80%–90% for intensity $>10^{19}\ \mathrm{W\,cm^{-2}}$.

DOI: 10.1103/PhysRevLett.102.045008 PACS numbers: 52.57.Kk, 52.38.Fz, 52.38.Kd

In the fast ignition concept [1] intense short-pulse laser light interacts with a dense plasma surrounding the compressed fuel, to produce a relativistic electron beam. This beam must propagate through the dense plasma and deposit its energy in the fuel, to produce an ignited propagating burn wave. The conversion efficiency of the laser energy into the electron beam energy is an important factor together with the beam temperature and its collimation and transport.

Experiments [2] in which the laser pulse is incident on a planar solid target indicate that the hot-electron temperature T_h is given by

$$T_h\ (\mathrm{keV}) = 215(I_{18}\lambda_{\mu\mathrm{m}}^2)^{1/3} \tag{1}$$

for a 1 μm laser wavelength with intensity I_{18} (in units of $10^{18}\ \mathrm{W\,cm^{-2}}$) in the range 0.03–6 giving a hot-electron temperature of 70–400 keV. These results are derived from x-ray bremsstrahlung measurements. It might appear from the scaling that this is resonance absorption, but the factor in front is about 3.5 times that of resonance absorption. Furthermore, with high contrast laser pulses, it may be possible to minimize preplasma production associated with laser prepulse, in which case the laser will be incident on an overdense plasma for which resonance absorption does not apply. More recent experiments [3,4] confirm that the one third scaling extends to higher intensity ($>10^{20}\ \mathrm{W\,cm^{-2}}$), which is a much weaker scaling than the ponderomotive scaling found in particle-in-cell (PIC) simulations [5].

In this Letter a theoretical model is developed which treats the laser-solid interaction region as a one-dimensional "black box" the thickness of which is a few collisionless skin depths. Fully relativistic conservation equations are applied to this, rather in the same way as in a shock transition, but here the entropy production is due to nonadiabatic electron motion. It assumes 100% laser-light absorption. This model gives a T_h scaling which agrees to a good approximation with the $(I\lambda^2)^{1/3}$ scaling over the appropriate intensity range. Next this is modified to include the effect of reflected light, which deposits twice the relevant photon momentum in the electrons, and makes the electron flux more beamlike. This extended model will show that laser absorption will reach 80%– 90% at high intensity. Essentially this theory gives an upper bound to the hot-electron temperature and to the reflectivity in the absence of any preformed plasmas.

In a fully relativistic regime, a "black box" model is developed in which both energy and momentum flux are conserved. There is an analogy here with the development of the Rankine-Hugoniot relations in shock physics, where the application of conservation laws each side of a black box at rest in the shock frame leads to robust results, independent of the detailed nonlinear transport processes occurring within the shock thickness. In the present case the thickness of the black box is a few collisionless skin depths. The one-dimensional energy flux conservation is

$$I = n_h m_e(\gamma_h - 1)v_z c^2 = n_c p_z(\gamma_h - 1)c^2, \tag{2}$$

while the momentum flux conservation is

$$\frac{I}{c} = n_h p_z v_z = \frac{n_c p_z^2}{m_e}, \tag{3}$$

where p_z, the forward relativistic electron momentum, is $m_e\gamma_h v_z$. Here the laser intensity is related to the dimensionless magnetic potential a_0 by

$$I = \frac{2\pi^2 m_e^2 c^3 a_0^2}{\mu_0 e^2 \lambda^2}, \tag{4}$$

where λ is the vacuum laser wavelength. The nonrelativistic critical density n_c is given by

$$n_c = \frac{4\pi^2 m_e}{\mu_0 e^2 \lambda^2}, \tag{5}$$

and it is assumed that the number density of the hot electrons n_h corresponds to the relativistic critical density of the hot electrons given by

$$n_h = \gamma_h n_c. \tag{6}$$

This implies that within the black box there is a density gradient, and the density in the laser-plasma interaction region is less than the peak (for example, solid) density. Equations (2) and (3) are consistent with the relativistic motion of a free electron in a plane electromagnetic wave,

$$\frac{p_z}{m_e c} \equiv \hat{p}_z = \gamma_h - 1. \tag{7}$$

Now γ_h depends on the total velocity of an electron. To obtain the hot-electron temperature a transformation to the axial rest frame of the electron beam is made, in which the total energy of an electron is E_0, given by

$$E_0^2 = E^2 - p_z^2 c^2 = m_e^2 c^4 \left[\left(1 + \frac{p_z}{m_e c} \right)^2 - \frac{p_z^2}{m_e^2 c^2} \right] = m_e^2 c^4 \left[1 + \frac{2 p_z}{m_e c} \right]. \tag{8}$$

On equating E_0 to $m_e \gamma_0 c^2$ and because the transverse momenta (p_x and p_y) are unaffected by the transformation, the hot-electron temperature T_h (in electron volts) can be considered to be

$$eT_h = m_e c^2 (\gamma_0 - 1) = m_e c^2 \left\{ \left[1 + \frac{2}{m_e c} \left(\frac{m_e I}{n_c c} \right)^{1/2} \right]^{1/2} - 1 \right\}. \tag{9}$$

In terms of dimensionless parameters, $t_h \equiv eT_h / m_e c^2$ and a_0, Eq. (9) can be written as

$$t_h = (1 + 2^{1/2} a_0)^{1/2} - 1. \tag{10}$$

This is the same as the electron temperature in the laboratory frame defined by $t_h = (1 + \hat{p}_\perp^2)^{1/2} - 1$, where $\hat{p}_\perp = p_\perp / m_e c$; i.e., t_h obtained in Eq. (10) for the rest frame is also valid for the laboratory frame as transverse momenta are unaffected by the transformation. It further implies that the cone angle of the hot-electron trajectories is $\tan^{-1}(8^{1/4}/a_0^{1/2})$.

This contrasts with the ponderomotive scaling found by Wilks *et al.* [5] for a PIC simulation, namely,

$$t_h = (1 + a_0^2)^{1/2} - 1. \tag{11}$$

The experimental scaling in Eq. (1) can be approximated to

$$t_h \approx 0.47 a_0^{2/3}. \tag{12}$$

These three scaling laws are plotted in Fig. 1 together with the latest experimental data points at high laser intensities reported in Refs. [3,4]. It can be seen that Eqs. (10) and (12) agree to within 30% over the range $0.28 < a_0 < 28.47$ [i.e., $1 \times 10^{17} < I\ (\mathrm{W\,cm^{-2}}) < 1 \times 10^{21}$] and intersect at $a_0 = 0.43$ and 180.2.

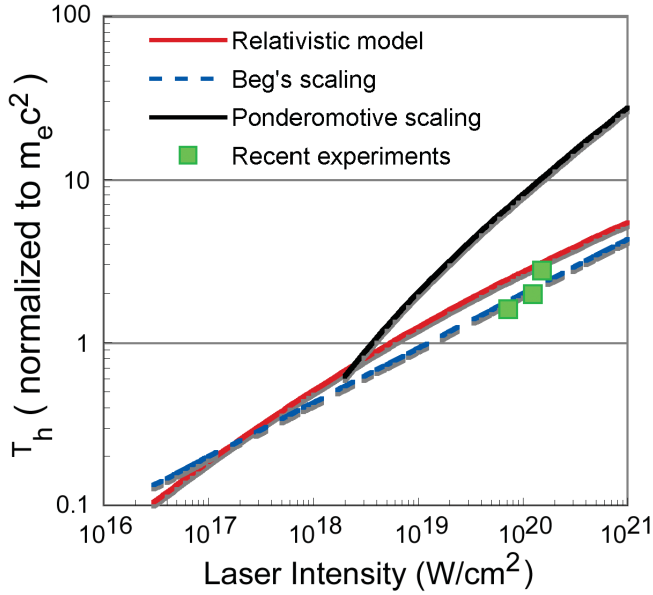

FIG. 1 (color). Plots of the dimensionless hot-electron temperature T_h (normalized to $m_e c^2$) versus laser intensity obtained in our relativistic model (red line) given by the new scaling Eq. (9); ponderomotive scaling (black line) in Ref. [5] [Eq. (10)]; Beg's experimental scaling (blue dashed line) [2] [Eq. (1)], and the recent experimental data at higher intensities (green squares) in Refs. [3,4].

The *total* electron kinetic energy K in the laboratory frame including the beam directed energy is

$$K = m_e c^2 (\gamma_h - 1) = m_e c^2 a_0 / 2^{1/2}. \tag{13}$$

Next the effect of reflected or backscattered laser light is considered. When light is reflected by a massive mirror, twice the photon momentum is deposited on the mirror. In the case here the electrons act as the mirror, indeed an accelerating mirror. Any subsequent transfer of momentum to the ions is through a combination of electric field, caused for instance by charge separation, and frictional drag with the cold electrons. [In the case of normal plasma ablation in low intensity laser interactions with a capsule, it is dominantly the frictional drag with the cold return current (i.e., the thermal force) which drives the ion ablation [6].] The extension of this Letter to include ion motion and electron transport including the return cold current and the possibility of anomalous resistivity is beyond the scope of the present study and probably not relevant to the laser-plasma interaction in the "black box."

The accelerating electrons which cause the reflection are moving finally in the forward direction, and ejected in bunches due to the $J \times B$ force at a frequency of 2ω. But they are replaced by electrons of higher number density constituting the return current, which move into the interaction volume. Considering the ions to be relatively massive it is reasonable to assume that on average the electrons that are involved in reflecting the light have no net motion in the z direction, since the net current density is to a good approximation zero.

If the absorbed fraction is $\alpha_{\rm abs}$, energy flux conservation now becomes

$$I - (1 - \alpha_{\rm abs})I = n_c p_z(\gamma_h - 1)c^2, \tag{14}$$

while momentum flux conservation is

$$\frac{I}{c} + (1 - \alpha_{\rm abs})\frac{I}{c} = \frac{n_c p_z^2}{m_e}. \tag{15}$$

Defining I_r as the reflected intensity,

$$I_r = (1 - \alpha_{\rm abs})I, \tag{16}$$

the combinations $c \times$ Eq. (15) $\pm$ Eq. (14) give

$$2I = n_c p_z c^2[p_z/m_e c + (\gamma_h - 1)] \tag{17}$$

and

$$2I_r = n_c p_z c^2[p_z/m_e c - (\gamma_h - 1)] \tag{18}$$

or, in dimensionless parameters,

$$i_i \equiv \frac{2I}{n_c p_z c^2} = \hat{p}_z + \gamma_n - 1 \tag{19}$$

$$i_r \equiv \frac{2I_r}{n_c p_z c^2} = \hat{p}_z - \gamma_h + 1, \tag{20}$$

where

$$\hat{p}_z \equiv p_z/m_e c. \tag{21}$$

As before, the energy in the rest frame of the electron beam, E_0, is found by the transformation

$$\begin{aligned} E_0^2 &= E^2 - p_z^2c^2 \\ &= (\gamma_h m_e c^2)^2 - p_z^2c^2 \\ &= m_e^2c^4(\gamma_h^2 - \hat{p}_z^2) \equiv m_e^2c^4\gamma_0^2. \end{aligned} \tag{22}$$

Hence the hot-electron temperature T_h as measured in the beam rest frame is now

$$\begin{aligned} t_h \equiv \frac{eT_h}{m_e c^2} &= \gamma_0 - 1 \\ &= [(\gamma_h + \hat{p}_z)(\gamma_h - \hat{p}_z)]^{1/2} - 1 \\ &= [(1 + i_i)(1 - i_r)]^{1/2} - 1. \end{aligned} \tag{23}$$

Equations (19) and (20) can be used to eliminate $\hat{p}_z$ to give

$$i_i + i_r = 2\hat{p}_z. \tag{24}$$

Defining r as i_r/i_i the relation

$$i_i = \frac{2^{1/2}a_0}{(1 + r)^{1/2}} \tag{25}$$

is found, leading to

$$t_h = \{[1 + 2^{1/2}a_0/(1+r)^{1/2}][1 - 2^{1/2}ra_0/(1+r)^{1/2}]\}^{1/2} - 1. \tag{26}$$

It can easily be seen that Eq. (26) becomes Eq. (10) for $r = 0$, while for $r \neq 0$, t_h is reduced. A limit on the value of r can be deduced from the condition $t_h > 0$ which yields

$$f(r) \equiv (1 - r^2)(1 - r)/(2r^2) > a_0^2. \tag{27}$$

Noting that df/dr is negative for $0 < r < 1$, and further defining α as $f(r) \equiv \alpha^2 a_0^2$ where $\alpha > 1$, t_h becomes

$$t_h = \{[1 + (1 - r)/(\alpha r)][1 - (1 - r)/\alpha]\}^{1/2} - 1. \tag{28}$$

Using r $(0 < r < 1)$, and α $(\alpha > 1)$ as parameters, the relationship between a_0 and the reflection coefficient, $\alpha_{\rm refl} = 1 - \alpha_{\rm abs} = r$, and α is given by

$$a_0^2 = \frac{(1 - r^2)(1 - r)}{2r^2\alpha^2}. \tag{29}$$

For example, this leads to $r < 0.1$ for $a_0^2 = 44.55$ (i.e., at $I = 6 \times 10^{19}$ W cm^{-2}). Table I gives $f(r)$ and $t_h(\alpha)$ for three values of α. For a given value of a_o^2 (i.e., intensity), $f(r)$ must be larger than this as shown in Eq. (27), leading to a maximum value of the reflectivity r. For example, for $a_0^2 = 44.55$, i.e., $I = 6.24 \times 10^{19}$ W cm^{-2}, r is required to be less than 0.1. The value of t_h then lies between 0 and that given by Eq. (10), i.e., $t_h = 2.23$, for which the parameter α ($>$1) could be useful.

Thus at high intensities the fraction of laser-light energy that is absorbed can exceed 90%. Recently, Ping *et al.* [7] reported high absorption efficiencies of 80%–90% at the laser intensities of 3×10^{20} W cm^{-2} with 45° incident angle (just a little smaller than predicted by this idealized model).

To obtain an understanding of why the hot-electron temperature can be far less than that given by ponderomotive scaling, it is instructive to examine the relativistic motion of a free electron in a sinusoidal plane-polarized electromagnetic wave, $\tilde{E}_0 \sin(\omega t - kz)$, and to use dimensionless proper time $s = \omega \int_0^t \gamma^{-1} dt$. With boundary con-

TABLE I. Calculated values of $f(r)$ and t_h (r, α) for various r.

r	0.1	0.2	0.3	0.4	0.5	0.6	0.7	0.8	0.9	1.0
$f(r)$	44.5	9.6	3.539	1.575	0.75	0.3556	0.156	0.0563	0.0117	0
$t_h(\alpha = 1.1)$	0.2921	0.1245	0.0654	0.0365	0.0204	0.010 95	0.0053	0.002 06	0.000 46	0
$t_h(\alpha = 1.2)$	0.4577	0.2019	0.1076	0.0607	0.034 14	0.018 35	0.008 89	0.003 47	0.000 77	0
$t_h(\alpha = 2)$	0.7393	0.3416	0.1867	0.1068	0.060 66	0.032 80	0.015 94	0.006 23	0.001 39	0

ditions that $x = 0$, $dx/dt = 0$, $z = 0$, $dz/dt = 0$ at $t = 0$, the following trajectories are obtained,

$$\frac{\omega x}{c} = a_0(s - \sin s), \tag{30}$$

$$\frac{\omega z}{c} = a_o^2\left(\frac{3}{4}s - \sin s + \frac{1}{8}\sin 2s\right), \tag{31}$$

$$\omega t = s + a_0^2\left(\frac{3}{4}s - \sin s + \frac{1}{8}\sin 2s\right). \tag{32}$$

Equation (31) means that in a full period of the electromagnetic wave as seen by the electron chasing after it, i.e., at $s = 2\pi$, z is $\frac{3}{4}a_0^2\lambda$ where λ is the wavelength of the light. But in an overdense plasma the collisionless skin depth, c/ω_{pe}, is less than λ, and for $a_0 \gtrsim 1$ the electron will traverse a distance greater than the skin depth before seeing even a quarter of a wavelength; i.e., it will not acquire the full ponderomotive potential. Thus we can understand the t_h scaling of Eq. (10).

The collisionless skin depth δ is modified for a large amplitude electromagnetic wave. An estimate can be made by employing the trajectories and velocity in the limit of small s. The current density J_x can be equated to the change of B_y over δ, the value of s being determined by $z = \delta$, giving

$$\delta \approx \frac{c}{\omega_p}\left(\frac{\omega}{\omega_p}\right)^{2/3} a_0^{1/3} \quad \text{for } a_0 \gg 1, \tag{33}$$

where $\omega_p = n_h e^2/m_e\varepsilon_0$.

It has been assumed that the laser light is incident on an overdense plasma. However, if there is a precursor laser pulse producing an underdense plasma, the electrons here will attain the full ponderomotive potential, leading to a tail in the distribution function with a higher temperature. Could such a precursor plasma of density ρ be swept up by the main laser pulse? The velocity attained is $\sim(I/\rho c)^{1/2}$, which for $I = 10^{23}\ \mathrm{W\,m^{-2}}$, ion number density of $10^{26}\ \mathrm{m^{-3}}$ with atomic number 27, leads to a displacement of 8.6 μm in 1 ps.

Lastly, a 2D effect can be estimated, namely, the azimuthal magnetic field B_θ generated due to the curl of the electric field induced by the deposition of photon momentum in the focal spot. This field will grow on a subpicosecond time scale and saturate when the magnetic pressure equals the plasma pressure. From $B_\theta^2/2\mu_0 = n_h e T_h$ and Eqs. (5), (6), and (9), for a value of intensity of $9 \times 10^{19}\ \mathrm{W\,cm^{-2}}$, a magnetic field of 620 MG is found, in good agreement with experiment [8].

In summary, using a robust model of energy and momentum conservation a value of the hot-electron temperature has been found in agreement with Beg's experimental scaling [2] for a wide range of laser intensities. Inclusion of reflected laser light leads to an upper limit to the reflectivity and hot-electron temperature especially at high intensity.

The work was partially supported by the U.S. Department of Energy under Contracts No. DE-AC52-07NA27344 (ACE) and No. DE-FC02-04ER54789 (Fusion Science Center). Some of this work was carried out by M. G. H. while visiting LLE, University of Rochester, and he would like to thank Professor R. L. McCrory and Dr. R. S. Craxton for useful discussions.

*Corresponding author.

[1] M. Tabak *et al.*, Phys. Plasmas **1**, 1626 (1994).
[2] F. N. Beg *et al.*, Phys. Plasmas **4**, 447 (1997).
[3] C. D. Chen *et al.*, Rev. Sci. Instrum. **79**, 10E305 (2008).
[4] A. G. MacPhee *et al.*, Rev. Sci. Instrum. **79**, 10F302 (2008).
[5] S. C. Wilks *et al.*, Phys. Rev. Lett. **69**, 1383 (1992).
[6] H. Kho, D. J. Bond, and M. G. Haines, Phys. Rev. A **28**, 3156 (1983).
[7] Y. Ping *et al.*, Phys. Rev. Lett. **100**, 085004 (2008).
[8] U. Wagner *et al.*, Phys. Rev. E **70**, 026401 (2004).